Constraining the timing of lobate debris apron emplacement at Martian mid-latitudes using a numerical model of ice flow Reid A. Parsons[1], Francis Nimmo[1], and Hideaki Miyamoto[2], [1]University of California, Santa Cruz, (rparsons@pmc.ucsc.edu) [2]University of Tokyo, Japan

Introduction: Lobate Debris Aprons (LDAs) surrounding plateaus, massifs, and valley walls at mid-latitudes are a present day reservoir of ice in the Martian near-surface [1, 2, 3]. These features raise questions about recent climate change on Mars due to the geographic coincidence of LDAs with other young water and ice-related features such as a mid-latitude mantling unit [4], gullies [5], and viscous flow features [6]. The shallow radar (SHARAD) on board Mars Reconnaissance Orbiter suggests LDAs contain relatively pure ice with thicknesses ranging from 300 to 700 m [3, 7]. These new findings place constraints on the ice rheology and provide an opportunity to constrain the timing of recent glaciation on Mars using numerical models of ice flow.

Observations: Debris aprons up to 800 m thick and 30 km long emanate from the 1-2 km high scarps surrounding mesas in Deuteronilus Mensae [8]. Studies using Mars Global Surveyor data sets have used the shape and distribution of aprons to constrain the rheology of the material making up these deposits [9, 10]. Mars Orbiting Laser Altimeter profiles of LDA surfaces show that they are gently sloping at $\sim$ 1°-4° with distal margins that steepen to up to 7° [10].

The presence of a buried reflector in published radargrams [3, 7] suggests deposits of massive ice $\sim$400 m thick have flowed outward from adjacent massifs. In addition to the ice thickness, the strength of the reflected signal recorded by SHARAD constrains the fraction of rocky material to be less than 10% within the LDA deposit [3].

Northern mid-latitude LDA thickness and length measurements are shown by the circles in Figure 1b [11]. The filled circles indicate LDAs with topographic profiles that are indicative of the presence of ice (oversteepened flow fronts, and a parabolic topographic profile). The three starred circles are LDAs whose surface age was estimated using crater age dating based on crater size-frequency measurements [11, 12].

Numerical Model: Our simple glacial flow model simulates changes in ice thickness, h, as ice flows outward over a flat surface. We base our approach on [13] which describes the viscous flow of a non-Newtonian fluid induced by pressure gradients associated with thickness variations. First, the shear stress (τ) and strain rate ($\dot{\epsilon}$) for a non-Newtonian fluid on a shallow slope are:

$$\tau(z) = \rho g(h-z)\left(\frac{\partial h}{\partial x} + \sin\theta\right) \quad (1)$$

$$\dot{\epsilon} = \frac{\partial v}{\partial z} = 2A\tau^n \quad (2)$$

where v is velocity in the x direction and n is the stress exponent. The parameters and their values are given in Table 1. z and x are coordinate directions where z is perpendicular to the slope and points upward ($z = 0$ at base of ice), and x is parallel to the sloping surface and points downslope. In our initial model, we use a value of $n = 3$ based on deformation experiments using applied stresses ranging from 0.1 to 1 MPa [14, 15]. A is a rheological parameter inversely related to viscosity. In our model we decompose A into

$$A = A_o e^{\left(\frac{-Q(T_m-T)}{RT_mT} - \phi b\right)} \quad (3)$$

where A_o is an adjustable value which controls the ice viscosity ($A_o = 10^{-24}$ Pa^{-n}s^{-1} gives a viscosity of 10^{14} Pa s at 0.1 MPa and T_m =273 K, appropriate for clean ice with a 1 mm grain size) [16, 17]. The exponential denotes viscosity variations due to temperature and dust fraction. Q is the activation energy at temperatures <255 K, R is the ideal gas constant, T is the local temperature, T_m is 273 K, ϕ is the dust fraction, and b is a constant [18].

Table 1 Definitions and measured or theoretical values (or range of values) for parameters used in the numerical simulations

Description	Symbol	Value(s)
activation energy	Q	50 kJ mol^{-1}
viscosity @ T=273	$\frac{\tau}{\dot{\epsilon}}$	10^{14} $Pa\ s$
dust fraction	ϕ	<10%
dust frac. coeff.	b	8
density of creep layer	ρ	1.00−1.07 g cm^{-3}
slope	θ	0°
gravity	g	3.7 m s^{-2}

Combining equations 1 and 2 using $n = 3$, and integrating in the z direction gives the downslope velocity:

$$v(z) = 2A\left(g\rho\left(\frac{\partial h}{\partial x} + \sin\theta\right)\right)^3\left(-\frac{z^4}{4} + z^3h - \frac{3}{2}z^2h^2 + h^3z\right) \quad (4)$$

assuming that there is no basal slip ($v = 0$ at $z = 0$). Finally, combining equations 3 and 4 assuming mass conservation gives the rate of change in glacier thickness

$$\frac{\partial h}{\partial t} = \frac{2}{5}A_o g^3 e^{\frac{-Q(T_m-T)}{RT_mT}}\frac{\partial}{\partial x}\left[e^{-\phi b}\rho^3h^5\left(\frac{\partial h}{\partial x} + \sin\theta\right)^3\right] \quad (5)$$

Here the parameters that can potentially vary spatially, such as ϕ, h, and ρ (dependent on ϕ), are kept inside the derivative with respect to x. Note that the model assumes a laterally and vertically constant temperature, which is appropriate for relatively small values of h.

We ran five different simulations varying the total volume of ice in each case. The initial thicknesses were all set to 1 km based on the estimated ice sheet thickness during regional glaciation in the Amazonian [19].

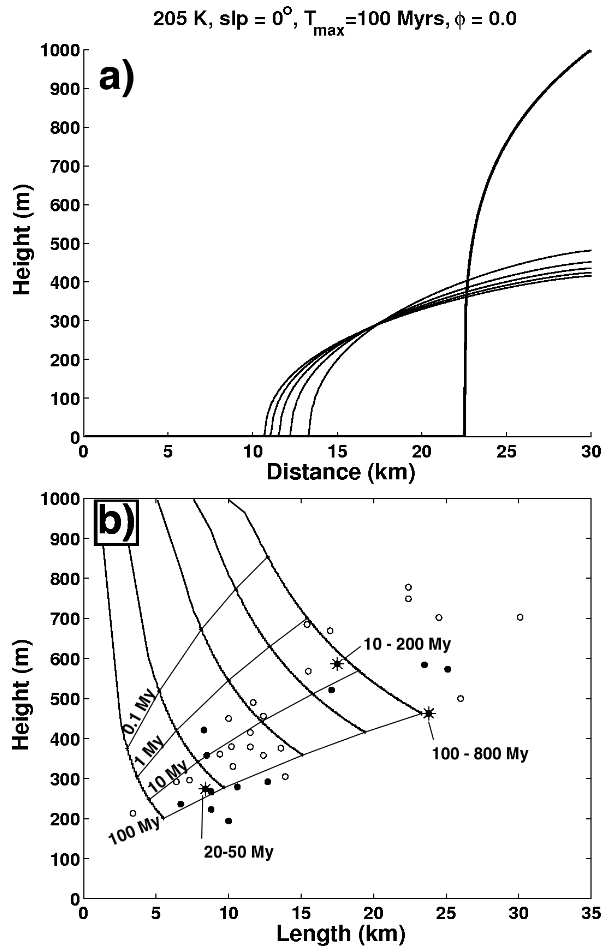

Figure 1 : a) Topographic profiles of an ice sheet initially 1 km thick and 7.5 km long with subsequent profiles plotted every 20 My. b) LDA height versus length measurements in the Deuteronilus Mensae region (open circles) with LDAs exhibiting a parabolic topographic profile shown with filled circles - three of these LDAs have approximate crater age date given (stars) [11]. Overlain are numerical model results of ice flow contoured by simulation time for 1 km ice deposits of different initial lengths.

Results: Figure 1a shows a 100 My simulation of ice flow for the ice deposit with an initial length of 7.5 km using an ice temperature of 205 K and $\phi = 0$. The initial profile is shown by the thick line with the thin lines indicating the topographic profiles at 20 My time intervals. Flow is initially fast due to the large ice thickness (see Equation 5), but significantly slows as the ice sheet thins.

The time-varying ice sheet thicknesses and lengths for the five runs are overlain on the data shown in Figure 1b. In all the simulations, the initial ice flow velocity is large resulting in a rapid decrease in thickness. Eventually the velocity slows as the ice deposits thin. Time contours are plotted on top of the simulations. These contours roughly follow the data indicating qualitative agreement with the observations if LDAs of different initial volumes flow over a 10 - 100 My timescale on a flat surface. These simulations assume dust-free ice (based on the radar observations) and an ice temperature of 205 K.

Annual mean surface temperature at $40°$ latitude is currently 205 K, and has varied between 205 and 195 K over the past 5 My [20]. We anticipate the warmest periods will control flow timescale due to the non-linear dependence of η on T. Based on energy balance calculations, the poles likely experienced more drastic temperature variations due to obliquity excursions than temperatures at mid and low latitudes. In the future we will explore how flow responds to variations in ϕ and obliquity-driven variations in T.

Conclusions: Simulations of dust-free ice-sheet flow over a flat surface at 205 K give LDA lengths and thicknesses that are in general agreement with observations in Deuteronilus Mensae if flow occurs over 10 - 100 My for ice sheets with initial lengths varying from 1 to 10 km and an initial thickness of 1 km. This range in LDA age is also in general agreement with a few LDAs that have crater age dates. If temperatures were warmer than 205 K in the past, then our results suggest LDAs should be younger than 100 My. However if mid-latitude temperatures were colder than 205 K in the past, or, if the dust content is higher than SHARAD suggests, then our suggested timescale for LDA flow is an underestimate.

References: [1]Colaprete, A. & Jakosky, B. 1998, J. Geophys. Res., 103, 5897. [2]Mangold, N. et al. 2002, Planet. and Space Sci., 50, 385. [3]Holt, S. et al. 2008, Science, 322, 1235. [4]Mustard, J., Cooper, C., & Rifkin, M. 2001, Nature, 412, 411. [5]Malin, M. & Edgett, K. 2000, Science, 288, 2330. [6]Milliken, R., Mustard, J., & Goldsby, D. 2001, Nature, 412, 411. [7]Plaut, J. et al. 2009, Geophys. Res. Let., 36, L02203, doi:10.1029/2008GL0363795. [8]Lucchita, B. 1984, Lunar Planet. Sci. Conf., XIV, suppl., B409 B418. [9]Mangold, N. & Allemand, P. 2001, Geophys. Res. Let., 28, 407. [10]Pierce, T. & Crown, D. 2003, Icarus, 163, 46. [11]Li, H., Robinson, M., & Jurdy, D. 2005, Icarus, 176, 382. [12]Hartmann, W. 2005, Icarus, 174, 294. [13]Nimmo, F. & Stevenson, D. 2001, J. Geophys. Res., 106, 5085. [14]Russell-Head, D. S. & Budd, W. F. 1979, J. Glaciol., 24, 117. [15]Glen, J. 1955, Proc. R. Soc. London, Series A, 228, 519. [16]Parsons, R. & Nimmo, F. 2009, J. Geophys. Res., 114, doi:10.1029/2007JE003006. [17]Goldsby, D. & Kohlstedt, D. 2001, J. Geophys. Res., 106, 11017. [18]Durham, W., Kirby, S., & Stern, L. 1992, J. Geophys. Res., 97, 20883. [19]Dickson, J., Head, J., & Marchant, D. 2008, Geology, 36, 411. [20]Schorghofer, N. 2008, Geophys. Res. Lett., 35, L18201, doi:10.1029/2008GL034954.